Nanoscale

PAPER

View Article Online
View Journal | View Issue

Cite this: *Nanoscale*, 2015, **7**, 13907

Mitochondria-acting hexokinase II peptides carried by short-length carbon nanotubes with increased cellular uptake, endosomal evasion, and enhanced bioactivity against cancer cells†

Sia Lee Yoong,[a] Wei Liang Lau,[b] Ang Yu Liu,[b] D'Arcy Prendergast,[b] Han Kiat Ho,[b] Victor Chun Kong Yu,[a,b] Chengkuo Lee,[c] Wee Han Ang*[a,d] and Giorgia Pastorin*[a,b,e]

Received 11th February 2015,
Accepted 12th July 2015

DOI: 10.1039/c5nr00980d

www.rsc.org/nanoscale

Type II hexokinase (HKII) has emerged as a viable therapeutic target due to its involvement in metabolic reprogramming and also apoptosis prevention. The peptide derived from the fifteen amino acid sequence in the HKII N-terminal region [HKII(pep)] can compete with endogenous proteins for binding on mitochondria and trigger apoptosis. However, this peptide is not cell-permeable. In this study, multi-walled carbon nanotubes (MWCNTs) were used to effectively deliver HKII(pep) across cellular barriers without compromising their bioactivity. The peptide was conjugated on either oxidized MWCNTs or 2,2′-(ethylenedioxy)bis(ethylamine)-functionalized MWCNTs, yielding MWCNT-HKII(pep) and MWCNT-TEG-HKII(pep), respectively. Both conjugates were shown to be internalized by breast cancer MCF-7 cells using confocal microscopy. Moreover, these nanoconjugates seemed to have escaped from endosomes and be in the vicinity of mitochondria. The WST-1 cytotoxicity assay conducted on MCF-7 and colon carcinoma HCT116 cells revealed that MWCNT–peptide conjugates were significantly more effective in curbing cancer cell growth compared to a commercially available cell permeable HKII fusion peptide. In addition, both nanoconjugates displayed an enhanced ability in eliciting apoptosis and depleting the ATP level in HCT116 cells compared to the mere HKII peptide. Importantly, hexokinase II release from mitochondria was demonstrated in MWCNT-HKII(pep) and MWCNT-TEG-HKII(pep) treated cells, highlighting that the structure and bioactivity of HKII(pep) were not compromised after covalent conjugation to MWCNTs.

1 Introduction

Hexokinase is an enzyme that phosphorylates glucose in an ATP-dependent manner and this commences the first committed step in glucose metabolism.[1] Among the four isozymes, only HKII possesses catalytically active N- and C-terminal halves. HKII binds onto the outer mitochondrial membrane (OMM) *via* its hydrophobic N-terminal region.[2] The voltage dependent anion channel (VDAC, also called the porin), which forms the major channel for the exchange of metabolites and ions between mitochondria and other cellular compartments, was identified to be the protein interacting with HKII on the OMM.[3]

HKII is abundantly found in embryonic tissues and to a lesser extent in certain adult tissues, such as adipose, skeletal muscles, and cardiac muscles.[1] Intriguingly, malignant tumours (lung cancer, breast cancer, colon cancer, *etc.*) exhibiting a highly glycolytic phenotype express higher levels (>100-fold) of HKII compared to normal cells.[4,5] In such tumours, mitochondrial HKII activity is also elevated.[6] As a result, these cells are able to survive and grow better in an oxygen-deprived environment inflicted by neoplastic mass accrual.[7]

HKII engages with four other partner proteins in aggravating the production of glucose-6-phosphate, which not only serves as a precursor of glycolysis but also functions as an intermediate for biosyntheses necessary for cancer cell proliferation. The four partner proteins include the plasma

[a]*NUS Graduate School for Integrative Sciences and Engineering, Centre for Life Sciences (CeLS), 28 Medical Drive, Singapore 117456, Singapore*
[b]*Department of Pharmacy, National University of Singapore, 3 Science Drive 2, Singapore 117543, Singapore. E-mail: phapg@nus.edu.sg; Fax: +65-67791554; Tel: +65-65161876*
[c]*Electrical and Computer Engineering, National University of Singapore, Engineering Drive 3, Singapore 117576, Singapore*
[d]*Department of Chemistry, National University of Singapore, 3 Science Drive 2, Singapore 117543, Singapore. E-mail: chmawh@nus.edu.sg; Fax: +65-67791691; Tel: +65-65165131*
[e]*NanoCore, Engineering Block A, Faculty of Engineering, National University of Singapore, Singapore 117576, Singapore*

† Electronic supplementary information (ESI) available: Additional TEM images, UV-Vis scanning characterisation, WST-1 assay results, and immunoblotting of HKII in the total cell lysate. See DOI: 10.1039/c5nr00980d

membrane glucose transporter, VDAC, adenine nucleotide translocase (ANT) and ATP synthase at the inner mitochondrial membrane (IMM). Apart from that, HKII association with VDAC has been shown to ingeniously desensitize tumour cells from cell death activation. It prevents proapoptotic Bcl-2 family members such as Bax and Bak from binding to mitochondria and this maintains mitochondrial integrity.[8] Targeted disruption of this association strongly induces cytochrome *c* release from mitochondria and apoptosis.[9]

Collectively, HKII represents a valuable therapeutic target for cancer therapy given its high expression level in cancer cells and engagement in the development of malignancy.[1] Compounds such as 3-bromopyruvate, clotrimazole and methyl jasmonate have been investigated *in vitro* and *in vivo* over the past few years for their anti-cancer properties *via* inhibition of HKII binding to mitochondria.[10] Since these small molecule compounds can also trigger other cytotoxic mechanisms, the contribution of HKII inhibition in their cytotoxicity remains debatable.[11–13] Peptides corresponding to the N-terminal fifteen amino acids of HKII [HKII(pep)] have thus been employed as selective dissociating agents for HKII binding on mitochondria to elicit apoptosis.[8,9,14,15] Being impermeable to cells, they are generally conjugated to an internalization peptide sequence, often known as the cell penetrating peptide (CPP), such as HIV-1 TAT or Drosophila Antennapedia, to facilitate cellular uptake. However, conjugation with CPP is unavoidably challenged by possible degradation (both extracellular and intracellular)[16] and endosomal entrapment.[17]

Nanocarriers have been employed to shield peptides against rapid peptidolysis and to selectively deliver them to cells *via* "passive" accumulation through the Enhanced Permeability and Retention (EPR) effect or "active" targeting by molecular recognition to designated sites.[18,19] Carbon nanotubes (CNTs) have emerged as a highly attractive nanodelivery system for several reasons. Firstly, their high ratio of length to diameter (aspect ratio) allows cellular entry *via* transmembrane penetration,[20] therefore bypassing endosomal entrapment and degradation.[21] Secondly, CNTs' surface can be functionalized with different bioactive species for both targeting and imaging purposes.[22] Surface modification through suitable functional groups can directly improve their aqueous suspendability and reduce their intrinsic cytotoxicity.[23,24] As a matter of fact, CNTs have already been demonstrated in numerous studies as useful nanocarriers for different classes of drugs,[25,26] including bioactive peptides.

In one study, a model penta-peptide and an antigenic epitope from the foot-and-mouth disease virus (FMDV) were covalently conjugated on single-walled carbon nanotubes (SWCNTs).[27] The FMDV peptide–SWCNT conjugate was shown to display an intact peptide's structure and could be recognized by monoclonal and polyclonal antibodies. Other FMDV peptides have also been coupled to mono- or bis-maleimido-derivatized SWCNTs using selective chemical ligation[28] and the epitopes were shown to be appropriately presented for recognition by antibodies. Notably, strong anti-peptide antibody responses were elicited when these peptide–SWCNT conjugates were administered to mice. In a more recent study, SWCNTs were employed as antigen carriers for poorly immunogenic Wilm's tumor protein (WT1) peptide 427 against hematopoietic malignancies.[29] WT1 peptide–SWCNT constructs were rapidly internalized *in vitro* into professional antigen presenting cells (APCs, mainly dendritic cells and macrophages) within minutes. Immunization of BALB/c mice with the peptide–SWCNT constructs mixed with an immunological adjuvant (TiterMax) induced specific IgG responses against the peptide, while the peptide alone or the peptide mixed with the adjuvant did not induce a comparable response. Notably, antibody responses to empty SWCNT carriers were not detectable *in vivo*.

To advance bioactive peptides for therapeutic application, it is necessary to develop an alternative delivery system to address issues pertaining to permeation across biological membranes, lysosomal entrapment, and peptidolytic degradation. Therefore, CNTs arise as a promising platform as exemplified by their remarkable capacity to effectively deliver antigenic peptides without compromising the peptide's structural integrity and display for target recognition. In this study, we set out to explore the delivery of the cytotoxic but non-cell-permeable peptide HKII(pep), which possesses intracellular targets on mitochondria, using CNTs. We aimed to improve its therapeutic efficacy against cancer cells and we have demonstrated for the first time that CNTs could serve as an excellent vehicle for bioactive HKII peptide delivery with enhanced efficacy over the commercially available CPP–HKII(pep) fusion peptide.

2 Results and discussion

2.1 Synthesis and characterization of MWCNT/HKII(pep) conjugates

Short-length MWCNTs (0.5–2 μm in length) were chosen as the peptide carrier due to their superior suspendability in aqueous solution and lower intrinsic cytotoxicity.[30,31] Oxidation treatment for 10 h was necessary to eliminate contaminants, further reduce the length to facilitate individualization of the CNTs and generate more carboxylic acid groups for peptide functionalization.[32] Fig. S1a and b† demonstrate significant reduction in their lengths after oxidation (100–500 nm), and confirmed that the structural integrity of the tubes was preserved. For loading of HKII(pep) on MWCNTs spaced with a linker, 2,2′-(ethylenedioxy)bis(ethylamine) (NH_2-TEG-NH_2) was conjugated onto MWCNT-COOH *via* an HATU-mediated amide coupling reaction. The amount of the loaded linker was estimated by the Kaiser test, which measures the concentration of the primary amine present on the linker. It was found that 446.9 μmol of $-NH_2$ groups was present on TEG-functionalized MWCNTs per gram of the sample. As HKII(pep) was conjugated *via* its N-terminal $-NH_2$ group, conversion of MWCNT-TEG into MWCNT-TEG-COOH was necessary (Scheme 1). Indeed, this reaction was proven to be successful, as denoted by the decrease in the Kaiser test value to

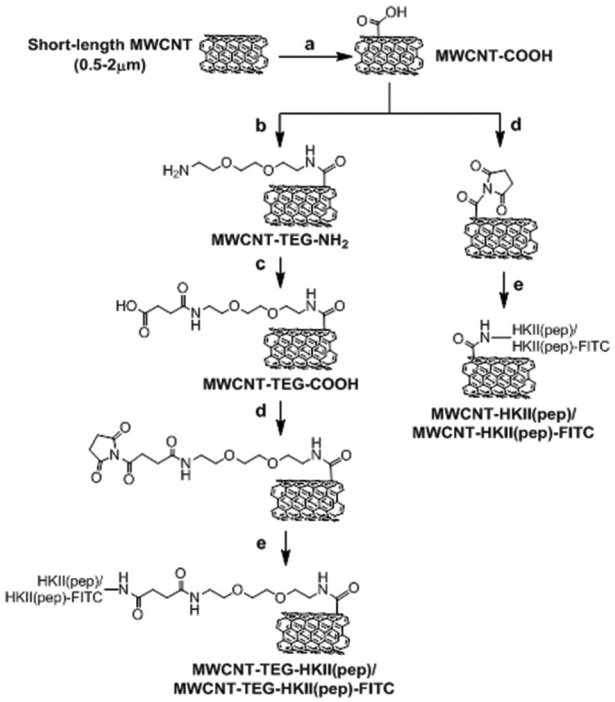

Scheme 1 Synthetic scheme for the fabrication of the CNT drug delivery system. (a) 98% sulphuric acid : 65% nitric acid = 3 : 1 v/v, 10 h; (b) (ethylenedioxy)bis-ethylamine, HATU, DIPEA, DMF, stirred at 40 °C, 12 h; (c) succinic anhydride, stirred at 40 °C, 12 h; (d) NHS, EDC, DMAP, DIPEA, DMF, stirred at 40 °C, 2 h; (e) HKII(pep)/HKII(pep)-FITC peptide, stirred at 40 °C, 72 h.

163.7 μmol g^{-1} for MWCNT-TEG-COOH (*ca.* 40%). Taking the difference of the Kaiser test values before and after reacting with succinic anhydride, the amount of –COOH converted was estimated to be 283.3 μmol g^{-1} for MWCNT-TEG-COOH, corresponding to approximately 60% of –COOH conversion.

HKII(pep) was loaded on MWCNT-COOH directly or MWCNT-TEG-COOH *via* amide coupling through its N-terminal $-NH_2$, giving rise to MWCNT-HKII(pep) and MWCNT-TEG-HKII(pep), respectively. After HKII(pep) conjugation, the peptide loading on MWCNTs was determined indirectly by measuring the residual unconjugated peptide amount before and after reaction using HPLC. The detection wavelengths were set at 230 nm and 280 nm, based on UV absorption of the peptide bond and phenylalanine residues (Fig. S2†). MWCNT-HKII(pep) and MWCNT-TEG-HKII(pep) were determined to be functionalized with *ca.* 208 μmol g^{-1} HKII peptide corresponding to *ca.* 37% w/w MWCNTs.

2.2 Cellular uptake of HKII(pep)-FITC functionalized MWCNTs

Confocal fluorescence microscopy was employed to investigate cellular uptake and determine the intracellular distribution of HKII(pep) conjugated MWCNTs. To visualize the location of the MWCNT conjugates, the HKII(pep) used was labelled with FITC *via* an additional lysine residue at the C-terminus [HKII-(pep)-FITC]. HKII(pep)-FITC was covalently conjugated on MWCNT-COOH and MWCNT-TEG-COOH in a similar fashion and added to MCF-7 cells for 6 h. The FITC labelled MWCNTs were tracked at 519 nm. The nucleus and the mitochondria were co-stained using Hoechst 33342 and MitoTracker® dyes, respectively.

Cells treated with HKII(pep)-FITC alone did not show an obvious green fluorescence signal in their intracellular space. On the other hand, MCF-7 cells incubated with MWCNT-HKII-(pep)-FITC or MWCNT-TEG-HKII(pep)-FITC displayed evident intensification of green fluorescence in intracellular space, indicating enhanced cellular uptake compared to HKII(pep)-FITC without a carrier (Fig. 1b and c). Notably, the presence of a linker between MWCNTs and HKII(pep)-FITC did not significantly alter cellular uptake and intracellular distribution of the whole conjugate. Importantly, the images revealed that both MWCNT constructs evaded from the endo-lysosome into the cytoplasm, unlike the free HKII(pep)-FITC. Nevertheless, it would be supplementary to include lysosomal staining to ascertain this inference.

When we compared the distribution of green fluorescence (FITC-labelled MWCNTs) and red fluorescence (mitochondria dye) in MWCNT-HKII(pep)-FITC and MWCNT-TEG-HKII(pep)-FITC treated MCF-7 cells (Fig. 1b and c), we observed that both fluorescent nanoconjugates seemingly colocalized with mitochondria (indicated by white arrows). This indicates the possibility that HKII(pep), after conjugation onto MWCNTs, was able to display its structure properly for target recognition on the OMM. Our findings echo with the report of the successful mitochondrial targeting of MWCNTs using a 25 amino acid long mitochondrial targeting signal peptide derived from the N-terminal region of human cytochrome *c* oxidase.[33] Although the major focus in that study was to target MWCNTs to mitochondria by functionalization with the signal peptide, we reason that the loaded peptide must have been displayed on MWCNTs properly for recognition by mitochondrial import receptors TOM70 and TOM20 on the OMM.[34] Hence, in our case, correct display of HKII(pep) on MWCNTs could have rendered an intracellular distribution pattern reflecting mitochondrial localization, similar to the reported HKII(pep) delivered by arginine based CPP.[9]

These findings validated our hypothesis that the functionalized MWCNTs could facilitate the cellular entry of HKII(pep). Importantly, MWCNT-HKII(pep)-FITC and MWCNT-TEG-HKII-(pep)-FITC were found to be in the vicinity of mitochondria, which prompted us to investigate whether such a phenomenon would be harnessed to improve efficacy *in vitro*.

2.3 Cytotoxicity assay of HKII(pep)-functionalized MWCNTs

In light of the promising findings from the cellular uptake study, we proceeded to evaluate the efficiency of HKII(pep) conjugated MWCNTs in eliciting toxicity in cancer cells. A two-way ANOVA was conducted to examine the effect of varying concentrations in different treatments, namely HKII(pep), commercially available cell permeable HKII(pep) [CPP-HKII-(pep)], MWCNT-HKII(pep), MWCNT-TEG-HKII(pep), on cell

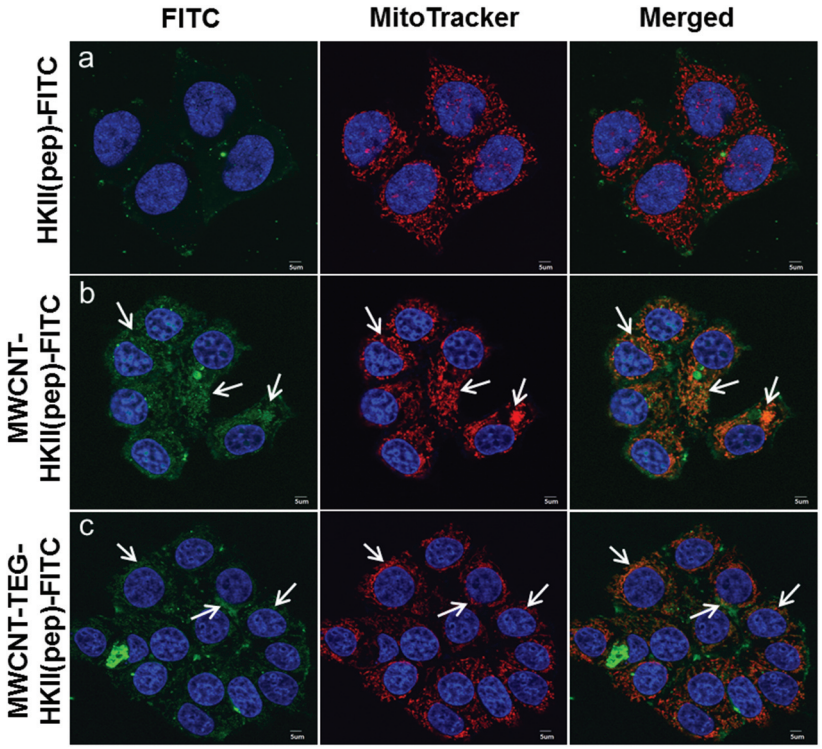

Fig. 1 Confocal images of MCF-7 cells incubated with 25 μM HKII(pep)-FITC, 50 μg mL^{-1} MWCNT-HKII(pep)-FITC, or 50 μg mL^{-1} MWCNT-TEG-HKII(pep)-FITC. Images showing green fluorescence indicate uptake of FITC labelled HKII(pep) or the corresponding nanoconjugates. Nuclei and mitochondria were stained with Hoechst 33342 (blue) and MitoTracker® Deep Red FM (red). Superimposed images are also shown (merge). Confocal images showed minute cellular uptake of HKII(pep)-FITC (first panel, a), while HKII(pep)-FITC carried by MWCNTs displayed enhanced cellular uptake (second (b) and third panel (c)). Similarity in the location of green [HKII(pep)-FITC on MWCNTs] and red fluorescence (mitochondria) is highlighted by white arrows.

survival. In MCF-7 cells, there was a statistically significant interaction between the effects of treatments and concentrations on cell survival, $F(6, 24) = 7.60$, $p = 0.0001$. Similarly, a statistically significant interaction was obtained in HCT116 cells between the effects of treatments and concentrations on cell survival, $F(6, 24) = 13.08$, $p < 0.0001$.

We found that HKII(pep) alone was not cytotoxic in cancerous MCF-7 and HCT116 cells, with at least 90% of cells being viable even after treatment with 50 μM of HKII(pep) for 48 h (Fig. 2). This was consistent with our findings obtained from confocal microscopy (Fig. 1a), which suggested that HKII(pep) alone was incapable of permeating the cell membrane and travel to its subcellular site of action. In contrast, simple main effect analysis showed that CPP–HKII(pep) was statistically more cytotoxic in MCF-7 cells across all concentration ranges (Fig. 2). Meanwhile in HCT116 cells, CPP–HKII(pep) was significantly more cytotoxic than HKII(pep) at 50 μM. This emphasizes the need of a permeability enhancer, in this case the internalization sequence of the Antennapedia homeoprotein, for realizing the cytotoxic activity of the HKII peptide that is, otherwise, "inert" to cells due to poor cellular internalization.

Growth inhibitory activity of MWCNT–peptide conjugates in HCT116 and MCF-7 cells was evaluated *via* WST-1 cytotoxicity assay.[35] Treatment with MWCNT-HKII(pep) and MWCNT-TEG-HKII(pep) resulted in a dose-dependent decrease in cell viability (Fig. 2a and b). Comparing CPP-HKII-(pep) with HKII(pep) carried by MWCNTs, HKII(pep)'s cancer cell killing efficacy was significantly enhanced using the MWCNT carrier according to simple main effect analysis. This is evidently pronounced in HCT116 cells in which both MWCNT constructs were significantly more cytotoxic than CPP–HKII(pep) at all concentrations (Fig. 2b). Notably, at a peptide concentration of 25 μM, more than 2-fold reduction in cell viability compared to CPP–HKII(pep) was observed in HCT116 cells when short-length MWCNTs were employed as the carrier. On the other hand, MCF-7 cells only retained 10% of cell viability after being treated with 50 μM MWCNT-HKII-(pep) or MWCNT-TEG-HKII(pep). This is significantly lower than *ca.* 40% survival in CPP–HKII(pep) treated cells. In short, we found that the HKII(pep) conjugated MWCNTs at 25 μM of peptide concentration exhibited a 50% improvement in cytotoxicity compared to HKII(pep) alone (Fig. 2). Additionally, HKII(pep) conjugated MWCNTs also compared favourably against the commercially available cell-permeable HKII fusion peptide carried by Antennapedia based CPP. This superiority over the peptide-based delivery system could be attributed to the fact that while CPP might not have precluded CPP–cargo

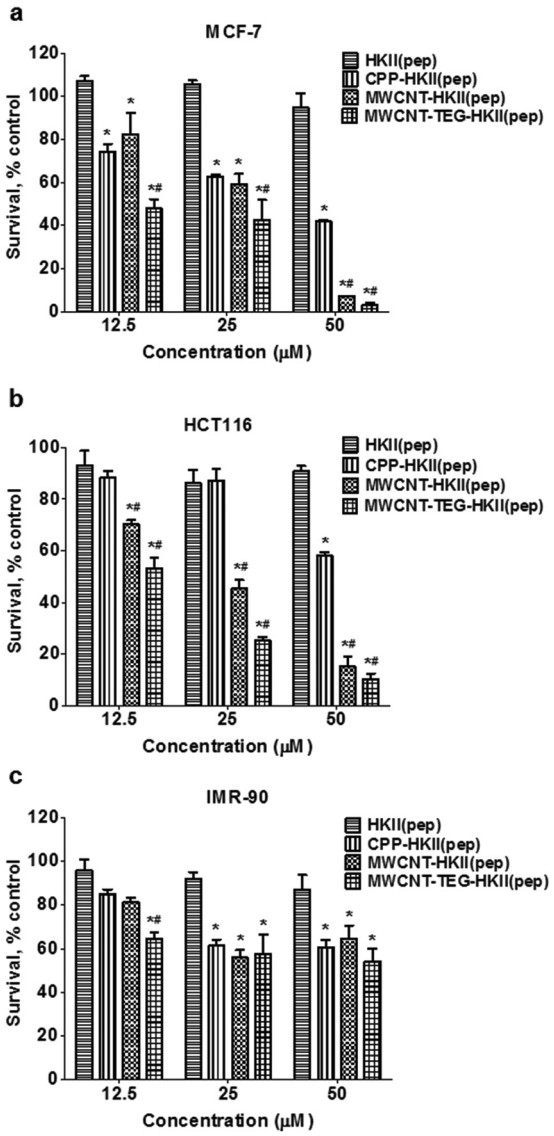

Fig. 2 Investigation of cell viability *via* MTT assay or WST-1 assay. HCT116, MCF-7, and IMR-90 cells were treated with 3 concentrations (12.5, 25, 50 μM) of HKII(pep); CPP-HKII(pep); MWCNT-HKII(pep); MWCNT-TEG-HKII(pep) for 48 h. The MTT assay was used to assess viability of cells treated with HKII(pep) and CPP-HKII(pep) while the WST-1 assay was used to assess viability of cells treated with MWCNT-HKII (pep) and MWCNT-TEG-HKII(pep). MTT/WST-1 readings from the control lane (*i.e.* cells without any treatment) were used as reference values for 100% survival. $^{*}P < 0.05$ compared to HKII(pep) based on two-way ANOVA and Bonferroni post analysis. $^{\#}P < 0.05$ compared to CPP-HKII(pep) based on two-way ANOVA and Bonferroni post analysis. For all panels, data represent three observations for each experiment and are expressed as mean ± S.E. ($n = 3$).

conjugates from being endocytosed and peptidolytically processed in lysosomes,[36] our MWCNT constructs explicitly evaded from endosomal entrapment and seemingly distributed to mitochondria (Fig. 1). Nevertheless, it would be intriguing to evaluate the stability of HKII(pep) conjugated MWCNTs in the presence of peptidase to confirm the role of MWCNTs as the protective peptide carrier.

In MCF-7 cells, a significant difference in cell survival was observed between MWCNT-HKII(pep) and MWCNT-TEG-(pep) treatment only at 12.5 μM. Meanwhile in HCT116 cells, MWCNT-TEG-HKII(pep) was more cytotoxic than MWCNT-HKII(pep) at 12.5 μM and 25 μM but not at 50 μM. Collectively we infer that the presence of linkers between MWCNTs and HKII(pep) does not impact the peptide's bioactivity. Moreover based on the observations from cellular uptake studies, it is apparent that the presence of a linker between MWCNTs and HKII(pep) does not affect intracellular distribution of the resulting constructs. We reason that as HKII(pep) contains fifteen amino acids, the presence of a mere 6-carbon TEG linker might be insignificant in decreasing steric hindrance. Nevertheless, it would be interesting to functionalize MWCNTs with cleavable linkers, *i.e.* disulfide-based or enzyme-sensitive linkers, for HKII(pep) delivery and compare the efficacy. Indeed, it was reported that the cytotoxicity of a covalently conjugated active moiety strongly depends on the type of cleavable linker used on MWCNTs.[37]

All the constructs were also tested in human fetal lung fibroblast IMR-90. A two-way ANOVA was also conducted to examine the effect of varying concentrations of different treatments on cell survival. The interaction between the effects of treatments and concentrations on cell survival was found to be statistically insignificant, $F(6, 23) = 1.52$, $p = 0.2165$. To our surprise, HKII(pep) coupled with a delivery carrier, be it either an Antennapedia-based internalization sequence or our MWCNT-based nanocarrier, exerted detectable toxic effects on this cell line, with *ca.* 40% reduction in cell viability at the highest tested concentration of 50 μM (Fig. 2c). This could be due to the considerable expression of HKII(pep) in this cell line, leading to the slight toxicity observed ensuing the entry of HKII(pep).[38] Nevertheless, the ability of HKII(pep) in deterring cancerous MCF-7 and HCT116 cell growth was still significantly more profound than its effect in IMR-90 cells. However, studies in other non-cancerous cell lines are essential to further confirm the selectivity towards cancer cells. If deemed necessary, active targeting by folic acid or RGD peptides could be devised on our MWCNT constructs to attain more preferential killing of cancer cells.[39]

To ascertain that the cytotoxicity observed with HKII(pep) conjugated MWCNT constructs was due to the activity of HKII-(pep) rather than the intrinsic toxicity of MWCNTs, we performed the WST-1 assay on cells exposed to the empty carrier (Fig. S3†). It was back-calculated from peptide loading that there was *ca.* 240 μg mL^{-1} of MWCNTs at the corresponding highest HKII(pep) concentration of 50 μM for both nanoconstructs (with or without a linker). We found that at the highest MWCNT concentration of 250 μg mL^{-1}, MWCNT-COOH did not elicit significant toxicity in HCT116, MCF-7, and IMR-90 cells with at least 80% of cells remaining viable (Fig. S3a†). On the other hand, treatment with 250 μg mL^{-1} MWCNT-TEG-COOH in all three cell lines resulted in *ca.* 40% drop in cell viability, signifying that the toxicity of MWCNT-TEG-COOH was higher than MWCNT-COOH. Nevertheless, compared to cells treated with HKII(pep) loaded MWCNT-TEG-HKII(pep)

that rendered less than 20% in viability, we conclude that the majority of the effect observed stemmed from the bioactivity of HKII(pep) rather than MWCNT-TEG-COOH's intrinsic cytotoxicity.

Together with the observations from confocal microscopy (Fig. 1b and c), these results implied that MWCNTs as the delivery system potentiated the efficacy of HKII(pep) primarily by increasing their availability inside the cells.

2.4 MWCNT-HKII(pep) and MWCNT-TEG-HKII(pep) depleted cellular energy and induced apoptosis

In malignant cancers with a highly glycolytic phenotype, after the rapid entry of glucose into cancer cells *via* the glucose transporter, HKII becomes the main facilitator for active glycolysis.[4] It binds to the OMM *via* VDAC, which, together with the ANT at IMM, transports ATP newly synthesized by ATP synthase (housed at the IMM) to HKII.[6] This positional advantage enables the enzyme to produce glucose-6-phosphate conveniently and leads to elevated glycolytic activity for production of building blocks and ATP to support tumour growth. In light of this, the intracellular ATP level was measured to examine if energy production in HCT116 cells was affected after exposure to HKII(pep) coupled to MWCNTs. Following addition of 25 μM of MWCNT-HKII(pep) or MWCNT-TEG-HKII(pep), the intracellular ATP level declined steadily after 2 h and further plunged with prolonged treatment (Fig. 3a). After 8 h of incubation with HKII(pep) conjugated MWCNTs, the cellular ATP level displayed a pronounced decrease to around 50%. On the contrary, incubation with either 25 μM HKII(pep), MWCNT-COOH, or MWCNT-TEG-COOH was unable to impact ATP metabolism in cells, demonstrated by the slight reduction in the ATP content.

On the other hand, the ability of HKII(pep) in inducing apoptosis was examined after its conjugation on MWCNTs. HCT116 cells were treated with 25 μM MWCNT-HKII(pep) or MWCNT-TEG-HKII(pep) or respective controls for 2 h. The ability of our constructs in eliciting apoptosis was validated by annexin V/PI staining. Apoptosis is distinguished from necrosis by characteristic morphological and biochemical changes, including compaction and fragmentation of the nuclear chromatin, shrinkage of the cytoplasm, and loss of the membrane asymmetry.[40] In apoptotic cells, phosphatidylserine is translocated from the cytoplasmic surface to the outer leaflet of the plasma membrane and the exposed phosphatidylserine is recognized by the human anticoagulant annexin V with high affinity.[41] Neither free HKII(pep) without a carrier, nor a plain carrier (MWCNT-COOH or MWCNT-TEG-COOH) induced apparent apoptotic events in HCT116 cells, as evidenced by the comparable extent of cell death with untreated control (Fig. 3b, first row). Conversely, 16.8% and 14.4% of MWCNT-HKII(pep) and MWCNT-TEG-HKII(pep) treated cells, respectively, manifested signs of early apoptosis indicated by a positive staining with Alexa Fluor® 488 conjugated Annexin V (Fig. 3b, bottom row). Concordant with previous findings in this report, both constructs of HKII(pep) carried by MWCNTs (with or without a linker) had no discernible difference in terms of peptide efficiency.

2.5 HKII(pep) conjugated on MWCNTs triggered HKII release from mitochondria

To validate if all the abovementioned effects of MWCNT-HKII-(pep) or MWCNT-TEG-HKII(pep) on HCT116 cells truly arose from the activity of HKII(pep), which is the ability to compete with HKII for binding on mitochondria, we carried out immunoblotting of the endogenous protein in the mitochondria-enriched fraction. Indeed, compared to untreated control, HCT116 cells treated with 25 μM of MWCNT-HKII(pep) or MWCNT-TEG-HKII(pep) exhibited diminished levels of HKII by *ca.* 40–50% in the mitochondria-enriched fraction. This implies that HKII(pep) on MWCNTs was capable of triggering HKII detachment from mitochondria (Fig. 4, lanes 3 & 4, respectively). In contrast, addition of bare HKII(pep) and empty MWCNT carriers did not result in significant loss of HKII from the mitochondria enriched-fraction (Fig. 4, lanes 2, 5 & 6).

This direct proof highlights the advantage of delivering the HKII peptide using MWCNTs without compromising its activity. Together with the observations in intracellular uptake and seemingly mitochondrial distribution, we infer that the conjugation of HKII(pep) on MWCNTs did not jeopardize the peptide display for target recognition. Moreover, we have demonstrated for the first time that the bioactive HKII peptide could be carried intracellularly by nanocarrier MWCNTs with higher cytotoxic effects on cancer cells compared to a conventional CPP delivery system. Essentially, the conjugated peptide was able to compete and displace endogenous HKII from its association with mitochondria. Our findings indicate the optimistic potential of developing MWCNTs as versatile nanocarriers for bioactive peptides.

3 Experimental

3.1 Materials

A fifteen amino acid N-terminal peptide sequence of HKII MIASHLLAYFFTELN [HKII(pep)] and its fluorescent derivative (modified with a fluorescein moiety at the additional lysine residue) with the sequence MIASHLLAYFFTELNK-FITC [HKII-(pep)-FITC] were purchased from Biomatik Corporation (De, USA). A commercially available cell-permeable peptide analogue of HKII (CPP-HKII) was procured from EMD Millipore (Darmstadt, Germany). Short-length MWCNTs were purchased from Nanostructured & Amorphous Materials Inc. (TX, USA). (Ethylenedioxy)bis-ethylamine (TEG), *N*,*N*-diisopropylethylamine (DIPEA), *N*-hydroxysuccinimide (NHS), 3-(4,5-dimethylthiazol-2-yl)-2,5-diphenyltetrazolium bromide (MTT), sucrose, (4-(2-hydroxyethyl)-1-piperazineethanesulfonic acid) (HEPES), potassium chloride (KCl), magnesium chloride ($MgCl_2$), ethylenediaminetetraacetic acid (EDTA), and ethylene glycol tetraacetic acid (EGTA) were procured from Sigma Aldrich (MO, USA). *O*-(7-Azabenzotriazol-1-yl)-*N*,*N*,*N*′,*N*′-tetra-

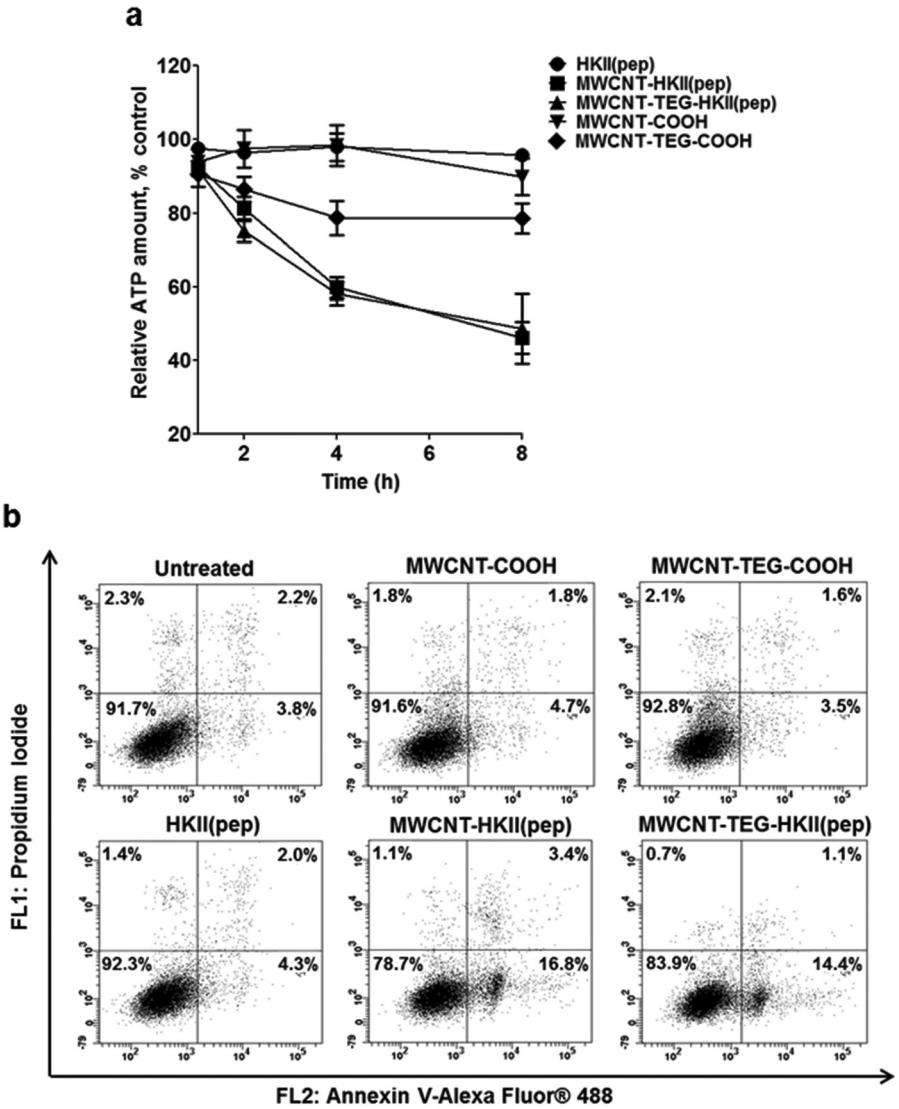

Fig. 3 (a) Quantitation of ATP levels in HCT116 cells after different treatments. HCT116 cells were treated with 25 μM HKII(pep); 25 μM MWCNT-HKII(pep); 25 μM MWCNT-TEG-HKII(pep); 125 μg mL^{-1} MWCNT-COOH; 125 μg mL^{-1} MWCNT-TEG-COOH for the indicated times. The intracellular ATP level was measured using the CellTiter-Glo Luminescent Cell Viability Assay kit. The points represent the mean ± S.E. (n = 3); (b) investigation of the mechanism of cell death after 2 h incubation of HKII(pep) (25 μM), MWCNT-HKII(pep) (25 μM), MWCNT-TEG-HKII(pep) (25 μM), MWCNT-COOH (125 μg mL^{-1}), or MWCNT-TEG-COOH (125 μg mL^{-1}) in HCT116 cells followed by annexin V/PI staining before analysing with flow cytometry. The left bottom quadrant represents live cells (annexin V/PI negative). The right bottom quadrant represents early apoptotic cells (annexin V positive/PI negative). The right upper quadrant represents necrotic/late apoptotic cells (annexin V/PI positive).

methyluronium hexafluorophosphate (HATU), 4-(dimethylamino)pyridine (DMAP) and 2,2′-diaminodiethyl disulfide dihydrochloride (cystamine) were purchased from Alfa Aesar (Lancaster, UK). 1-Ethyl-3-(3-dimethylaminopropyl)carbodiimide hydrochloride (EDC) was purchased from GL BioChem (Shanghai, China). Potassium cyanide (KCN) was kindly provided by the teaching lab of pharmacy department, National University of Singapore. Dulbecco's modified Eagle's medium (DMEM), fetal bovine serum (FBS), and protease inhibitor cocktail were procured from Thermo Scientific (MA, USA). RPMI-1640, McCoy's 5A medium, and TrypLE™ Express Enzyme were purchased from Life Technologies (CA, USA). 4-[3-(4-Iodophenyl)-2-4-(nitrophenyl)-2*H*-5-tetrazolio]-1,3-benzene disulfonate (WST-1) was purchased from Roche Applied Science (IN, USA). CellTiter-Glo Luminescence Cell Viability Assay kit was purchased from Promega Corp. (WI, USA). Dimethyl formamide (DMF) and dimethyl sulfoxide (DMSO) were obtained from Merck Millipore (Darmstadt, Germany). Bradford reagent was procured from Bio-Rad Laboratories Inc. (CA, USA). Antibodies to VDAC-1 (20B12) and HKII (C-14) were purchased from Santa Cruz Biotechnology Inc. (TX, USA).

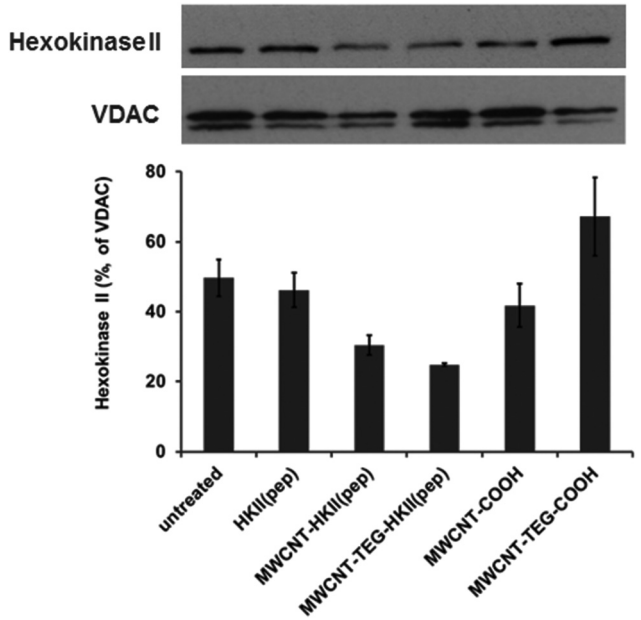

Fig. 4 Mitochondria extraction and immunoblotting of hexokinase II. HCT116 cells were treated with HKII(pep) (25 μM); MWCNT-HKII(pep) (25 μM); MWCNT-TEG-HKII(pep) (25 μM); MWCNT-COOH (125 μg mL^{-1}); MWCNT-TEG-COOH (125 μg mL^{-1}) for 4 h. Thereafter, the cells were harvested and crude extraction was performed to obtain the mitochondria-enriched fraction. Western blotting of HKII was performed in the mitochondria-enriched fraction and the immunoblot of VDAC served as loading control. Densitometry of each lane was quantitated using ImageJ (NIH, USA).

3.2 Functionalization of CNTs for peptide delivery

The synthetic scheme starting from the functionalization of the CNT carrier to the final attachment of HKII(pep) is summarized in Scheme 1. Pristine short-length MWCNTs (20 mg) were oxidized for 10 h by sonication in 98% sulphuric acid : 65% nitric acid (3 : 1 v/v, 4 mL) to create the carboxylic acid groups needed for subsequent functionalization. The oxidized MWCNTs were then purified and recovered, yielding MWCNT-COOH (19 mg).[42]

In order to add amine-terminated 2,2′-(ethylenedioxy)bis-(ethylamine) (TEG) groups, oxidized MWCNT-COOH (15 mg, 45 μmol of COOH) was reacted with TEG, yielding MWCNT-TEG-NH_2, according to a previous report.[42]

The conversion of the free terminal amino group present on the linker TEG into the COOH group allowed the HKII(pep) to be linked to the CNTs *via* its N-terminal amine. 8 mg of MWCNT-TEG-NH_2 were reacted with 30 equivalents of succinic anhydride and 2 equivalents of DIPEA in 1 mL of dry DMF. The reaction mixture was then stirred at 40 °C for 12 h. The eventual MWCNT-TEG-COOH was then harvested *via* filtering through a 0.2 μm PTFE membrane, and rinsed thoroughly with DMF, followed by methanol and DI water. The MWCNTs were subsequently recovered from the membrane with additional DI water and lyophilized, giving 7.5 mg of MWCNT-TEG-COOH. TEG loading on MWCNT-TEG-NH_2 and the conversion into –COOH were estimated by a quantitative Kaiser test.[42] Briefly, the primary amine on MWCNT-TEG-NH_2 would generate relatively higher Kaiser test readouts. As for MWCNT-TEG-COOH, the decrease in Kaiser test readouts represents the extent of conversion into a carboxylic acid.

3.3 Conjugation of HKII(pep)/HKII(pep)-FITC to MWCNTs

MWCNT-COOH and MWCNT-TEG-COOH were further functionalized with HKII(pep), yielding MWCNT-HKII(pep) and MWCNT-TEG-HKII(pep), respectively. Briefly, 5 equivalents of EDC·HCl, 5 equivalents of NHS and 2 μL of DIPEA were added into 0.5 mL of dry DMF in the presence of a catalytic amount of DMAP before addition of the CNTs. The reaction mixture was then stirred at 60 °C for 2 h. The resulting carboxylic acid activated MWCNTs were then filtered through a 0.2 μm PTFE membrane and washed 4 times with 100 μL of dry DMF. The MWCNTs were recovered from the membrane with 500 μL of dry DMF. Two equivalents of HKII(pep) were reconstituted in 500 μL of dry DMF with 4% DMSO. 10 μL of the reconstituted peptide solution was kept for HPLC analysis and the remaining solution was then added to the carboxylic acid activated MWCNTs in DMF and allowed to react at 40 °C for 72 h. The reaction mixture was then filtered through a 0.2 μm PTFE membrane, and rinsed thoroughly with DMF, followed by methanol and DI water. The filtrate and DMF washes were collected for subsequent HPLC analysis for estimation of peptide loading. The MWCNTs were recovered from the membrane with additional DI water and lyophilized.

HKII(pep)-FITC functionalization on MWCNT-COOH or MWCNT-TEG-COOH for confocal microscopy was performed similarly to the abovementioned HKII(pep) conjugation.

3.4 Estimation of peptide loading *via* HPLC

As MWCNTs could not be injected directly into a reversed phase HPLC C-18 column, estimation of peptide loading was carried out indirectly by subtracting the amount of unreacted peptide after reaction from the total peptide before the reaction. A calibration curve was constructed by injecting a series of calibration (standard) solutions of known HKII(pep) concentration and a standard graph with response (area under the curve) *versus* concentration was obtained. HKII(pep) solutions of different concentrations were prepared (3.5 mg mL^{-1}, 1.75 mg mL^{-1}, 0.88 mg mL^{-1}, 0.44 mg mL^{-1}, and 0.22 mg mL^{-1}). All the samples were analyzed using an Agilent 1200 Series HPLC System fitted with a Waters XTerra RP18 Column, 5 μm, 4.6 × 150 mm column. The analysis was conducted at a gradient of 35% acetonitrile (ACN)/65% H_2O to 65% ACN/35% H_2O in 10 min with a flow rate of 0.8 mL min^{-1}.

3.5 Cell culture

Human breast cancer cells MCF-7 and human colon carcinoma cells HCT116 were selected as cancer prototypes to evaluate the suitability of CNTs as the drug delivery system for bioactive HKII(pep) due to their reported usage in the HKII-related study.[15,43] Human fetal lung fibroblasts IMR-90 were

employed as the non-cancerous control. MCF-7, HCT116, and IMR-90 were purchased from ATCC (VA, USA) and maintained in RPMI 1640, McCoy's 5A, and DMEM, respectively. All media were supplemented with 10% FBS and the cells were incubated at 37 °C in humidified air containing 5% CO_2. All cells were sub-cultured every 3 to 4 days with TrypLE™ Express Enzyme.

3.6 Uptake and intra-cellular distribution of HKII(pep) functionalized MWCNTs

Confocal microscopy was conducted to investigate cellular uptake and intra-cellular distribution of HKII(pep)-FITC conjugated on MWCNT-COOH and MWCNT-TEG-COOH, respectively. Briefly, MCF-7 cells were seeded into a 29 mm glass bottom dish (In Vitro Scientific, USA) at a density of 5×10^4 cells per mL for 24 h, followed by incubation with 25 μM of HKII(pep)-FITC peptide, 50 μg mL^{-1} of MWCNT-HKII(pep)-FITC or MWCNT-TEG-HKII(pep)-FITC for 6 h. Thereafter, the cells were incubated with Hoechst 33342 (5 μg mL^{-1}) for 10 min as a nuclear counter-stain, followed by MitoTracker® Deep Red FM (25 nM) for 5 min to stain mitochondria before being viewed under a confocal microscope (Confocal Laser Scanning Biological Microscope FV10i, Olympus). HKII(pep)-FITC functionalized MWCNTs, MitoTracker® Deep Red FM, and Hoechst 33342 were excited at 495 nm, 635 nm, and 352 nm, respectively. Fluorescence emission was recorded at 519 nm, 690 nm, and 455 nm for HKII(pep)-FITC functionalized MWCNTs, MitoTracker® Deep Red FM, and Hoechst 33342, respectively.

3.7 Cytotoxicity assay

The MTT assay was used for experiments involving HKII(pep) and its cell-permeable analogue CPP-HKII(pep), while the WST-1 assay was employed for experiments involving CNTs, as CNTs could bind to the insoluble MTT formazan crystals and artificially lower the measured absorbance values.[35] WST-1 produces a water-soluble formazan product and is hence able to resolve this inaccuracy.

To perform the cytotoxicity assay, cells were first seeded in 96-well tissue culture plates (Costar, Corning NY) at a density of 1×10^4 cells per well for IMR-90 and HCT116, and 8000 cells per well for MCF-7. After 24 h, the medium was removed and the cells were exposed to varying concentrations of test compounds. HKII(pep) loading was used to calculate the amount of MWCNTs needed to prepare the corresponding test concentration of the peptide. After another incubation of 48 h, the medium was aspirated, replaced with 100 μL of either MTT (0.5 mg mL^{-1} in PBS) or WST-1 (1 : 15 dilution from ready-to-use stock in PBS), and incubated for 4 h or 30 min, respectively. For the MTT assay, the MTT solution was removed and DMSO was added to dissolve the insoluble purple formazan crystals. For the WST-1 assay, 80 μL of the WST-1 solution without cells or MWCNTs was aspirated for subsequent absorbance reading. The absorbance of the assayed solution was measured at 595 nm for MTT and 440 nm for WST-1 using a microplate reader (BioTek™ Synergy™ H1 Hybrid Multi-Mode Microplate Reader). Experiments were performed in three repeats for at least three replicates. The data were analyzed using GraphPad Prism (Version 6.0, GraphPad Software).

3.8 Apoptosis/necrosis staining and flow cytometry

For apoptosis/necrosis staining, HCT116 cells were seeded in a 12-well culture plate (SPL Life Sciences Co. Ltd, Korea) at 1×10^5 cells per well and allowed to grow for 72 h. The cells were then given different treatments for 2 h. All cells were harvested and stained at a density of 1×10^6 cells per mL with 2 μL of Alexa Fluor® 488 conjugated Annexin V and 0.1 μg of propidium iodide (PI) for 15 min at room temperature. All cell samples were immediately analyzed by flow cytometry using a BD LSRFortessa™ Flow Cytometry Analyser (BD Biosciences, USA). Alexa Fluor® 488 conjugated Annexin V was excited using a 488 nm laser and PI was excited using a 561 nm laser. Fluorescence emissions were recorded at 530 nm and 575 nm for Alexa Fluor® 488 conjugated Annexin V and PI, respectively.

3.9 ATP quantitation

HCT116 cells were seeded at 2×10^4 cells per well in a 96-well culture plate and allowed to grow for 48 h. Different treatments were given for 1 h, 2 h, 4 h, and 8 h. The ATP level in cells was then quantitated using a CellTiter-Glo Luminescent Cell Viability Assay kit according to the manufacturer's protocol. Luminescence was measured by using a BioTek™ Synergy™ H1 Hybrid Multi-Mode Microplate Reader from BioTek Instruments Inc. (VT, USA).

3.10 Mitochondria extraction and immunoblotting of HKII

Mitochondria isolation was performed as previously described.[44,45] Briefly, a total of 1×10^7 cells were resuspended in mitochondria isolation buffer (250 mM sucrose, 20 mM HEPES–NaOH [pH 7.9], 10 mM KCl, 1.5 mM $MgCl_2$, 1 mM EDTA, 1 mM EGTA) supplemented with protease inhibitor cocktail and disrupted by 20 strokes through a 25 gauge needle followed by centrifugation at 800*g* for 10 min at 4 °C. Supernatants were centrifuged twice at 12 000*g* for 20 min each at 4 °C to pellet the heavy membrane fraction enriched with mitochondria for the analysis of HKII. Immunoblotting was carried out as described.[46] The protein concentration of each sample was determined by the Bradford assay. An equal amount of proteins for each sample was subjected to fractionation on SDS-PAGE, followed by western blotting analysis for HKII and VDAC-1. Densitometry of each lane was quantitated using ImageJ (NIH, USA).

3.11 Statistical analysis

All experiments were performed in triplicate unless otherwise stated. The results of experimental repeats for cytotoxicity assay, intracellular ATP quantification, and western blot densitometry were input into GraphPad Prism 5 (Ca, USA) and the corresponding plot with mean and SEM was obtained. For the cytotoxicity assay, statistical significance was assessed using

two-way ANOVA comparing treatment groups [HKII(pep), CPP-HKII(pep), MWCNT-HKII(pep), MWCNT-TEG-HKII(pep)] and concentrations followed by *post hoc* analysis with the Bonferroni test with $p < 0.05$ considered significant. These statistical analyses were performed using GraphPad Prism 5.

4 Conclusion

Two different conjugates, MWCNT-HKII(pep) and MWCNT-TEG-HKII(pep), were successfully synthesized by amide coupling. Both constructs were internalized intracellularly and they displayed a considerably higher degree of cellular uptake compared to the peptide without a carrier. Notably, the tendency of both nano-conjugates to adopt an intracellular dissemination pattern resembling mitochondria distribution was observed. Cytotoxicity assays suggested that conjugation of HKII(pep) on MWCNTs with or without a linker did not hinder the peptide from exerting its bioactivity. 2-fold enhancement in peptide cytotoxic action was observed with HKII(pep) conjugated MWCNTs compared to commercially available CPP-HKII(pep). Moreover, the MWCNT delivery system was superior to commercially available CPPs in terms of efficacy enhancement. The MWCNT–peptide conjugates were able to elicit apoptosis and decrease the ATP level in cells. Importantly, HKII(pep) covalently conjugated on MWCNTs was shown to compete with endogenous HKII for binding onto mitochondria, emphasizing the immense potential of MWCNTs as effective nanocarriers for peptide delivery.

Acknowledgements

This research was supported by the National University of Singapore, Department of Pharmacy ((AcRF) Tier 1-FRC grant R-148-000-164-112) and by MOE of Singapore (grant MOE2011-T21-1201-P09; R-144-000-306-112). An NGS graduate fellowship is thankfully acknowledged by S. L. Y. for financial support of her graduate study. Also, we would like to thank NUHS flow cytometry laboratory, Ms Wang Xiaoning and Ms Toh Chin Min for support in flow cytometry experiments. Last but not least, the estimation of peptide loading by reversed phase HPLC analysis would not have been accomplished without the kind help from Ms Tang Shi Qing, Dr Pondy Murugappan Ramanujulu, Prof. Christina Chai, and Prof. Brian Dymock from the Department of Pharmacy.

References

1 J. E. Wilson, *J. Exp. Biol.*, 2003, **206**, 2049–2057.
2 D. Sui and J. E. Wilson, *Arch. Biochem. Biophys.*, 1997, **345**, 111–125.
3 J. G. Pastorino and J. B. Hoek, *J. Bioenerg. Biomembr.*, 2008, **40**, 171–182.
4 S. P. Mathupala, A. Rempel and P. L. Pedersen, *J. Biol. Chem.*, 2001, **276**, 43407–43412.
5 P. L. Pedersen, S. P. Mathupala, A. Rempel, J. F. Geschwind and Y. H. Ko, *Biochim. Biophys. Acta*, 2002, **1555**, 14–20.
6 S. P. Mathupala, Y. H. Ko and P. L. Pedersen, *Oncogene*, 2006, **25**, 4777–4786.
7 M. G. Vander Heiden, L. C. Cantley and C. B. Thompson, *Science*, 2009, **324**, 1029–1033.
8 J. G. Pastorino, N. Shulga and J. B. Hoek, *J. Biol. Chem.*, 2002, **277**, 7610–7618.
9 N. Majewski, V. Nogueira, P. Bhaskar, P. E. Coy, J. E. Skeen, K. Gottlob, N. S. Chandel, C. B. Thompson, R. B. Robey and N. Hay, *Mol. Cell*, 2004, **16**, 819–830.
10 S. Fulda, L. Galluzzi and G. Kroemer, *Nat. Rev. Drug Discovery*, 2010, **9**, 447–464.
11 S. Ganapathy-Kanniappan, M. Vali, R. Kunjithapatham, M. Buijs, L. H. Syed, P. P. Rao, S. Ota, B. K. Kwak, R. Loffroy and J. F. Geschwind, *Curr. Pharm. Biotechnol.*, 2010, **11**, 510–517.
12 E. Flescher, *Cancer Lett.*, 2007, **245**, 1–10.
13 D. D. Meira, M. M. Marinho-Carvalho, C. A. Teixeira, V. F. Veiga, A. T. Da Poian, C. Holandino, M. S. de Freitas and M. Sola-Penna, *Mol. Genet. Metab.*, 2005, **84**, 354–362.
14 F. Chiara, D. Castellaro, O. Marin, V. Petronilli, W. S. Brusilow, M. Juhaszova, S. J. Sollott, M. Forte, P. Bernardi and A. Rasola, *PLoS One*, 2008, **3**, e1852. Available from URL: http://www.ncbi.nlm.nih.gov/pmc/articles/PMC2267038/.
15 N. Shulga, R. Wilson-Smith and J. G. Pastorino, *Cell Cycle*, 2009, **8**, 3355–3364.
16 C. Palm, M. Jayamanne, M. Kjellander and M. Hallbrink, *Biochim. Biophys. Acta*, 2007, **1768**, 1769–1776.
17 A. Erazo-Oliveras, N. Muthukrishnan, R. Baker, T. Y. Wang and J. P. Pellois, *Pharmaceuticals*, 2012, **5**, 1177–1209.
18 N. R. Soman, S. L. Baldwin, G. Hu, J. N. Marsh, G. M. Lanza, J. E. Heuser, J. M. Arbeit, S. A. Wickline and P. H. Schlesinger, *J. Clin. Invest.*, 2009, **119**, 2830–2842.
19 C. Prego, D. Torres, E. Fernandez-Megia, R. Novoa-Carballal, E. Quiñoá and M. J. Alonso, *J. Controlled Release*, 2006, **111**, 299–308.
20 K. Kostarelos, L. Lacerda, G. Pastorin, W. Wu, S. Wieckowski, J. Luangsivilay, S. Godefroy, D. Pantarotto, J. P. Briand, S. Muller, M. Prato and A. Bianco, *Nat. Nanotechnol.*, 2007, **2**, 108–113.
21 Q. Mu, D. L. Broughton and B. Yan, *Nano Lett.*, 2009, **9**, 4370–4375.
22 S. M. Janib, A. S. Moses and J. A. MacKay, *Adv. Drug Delivery Rev.*, 2010, **62**, 1052–1063.
23 A. Bianco, K. Kostarelos and M. Prato, *Curr. Opin. Chem. Biol.*, 2005, **9**, 674–679.
24 M. Prato, K. Kostarelos and A. Bianco, *Acc. Chem. Res.*, 2008, **41**, 60–68.
25 B. S. Wong, S. L. Yoong, A. Jagusiak, T. Panczyk, H. K. Ho, W. H. Ang and G. Pastorin, *Adv. Drug Delivery Rev.*, 2013, **65**, 1964–2015.
26 S. Boncel, P. Zajac and K. K. Koziol, *J. Controlled Release*, 2013, **169**, 126–140.

27 D. Pantarotto, C. D. Partidos, R. Graff, J. Hoebeke, J. P. Briand, M. Prato and A. Bianco, *J. Am. Chem. Soc.*, 2003, **125**, 6160–6164.
28 D. Pantarotto, C. D. Partidos, J. Hoebeke, F. Brown, E. Kramer, J. P. Briand, S. Muller, M. Prato and A. Bianco, *Chem. Biol.*, 2003, **10**, 961–966.
29 C. H. Villa, T. Dao, I. Ahearn, N. Fehrenbacher, E. Casey, D. A. Rey, T. Korontsvit, V. Zakhaleva, C. A. Batt, M. R. Philips and D. A. Scheinberg, *ACS Nano*, 2011, **5**, 5300–5311.
30 K. Kostarelos, *Nat. Biotechnol.*, 2008, **26**, 774–776.
31 K. Kostarelos, A. Bianco and M. Prato, *Nat. Nanotechnol.*, 2009, **4**, 627–633.
32 W. Wu, R. Li, X. Bian, Z. Zhu, D. Ding, X. Li, Z. Jia, X. Jiang and Y. Hu, *ACS Nano*, 2009, **3**, 2740–2750.
33 A. Battigelli, J. Russier, E. Venturelli, C. Fabbro, V. Petronilli, P. Bernardi, T. Da Ros, M. Prato and A. Bianco, *Nanoscale*, 2013, **5**, 9110–9117.
34 T. Omura, *J. Biochem.*, 1998, **123**, 1010–1016.
35 J. M. Worle-Knirsch, K. Pulskamp and H. F. Krug, *Nano Lett.*, 2006, **6**, 1261–1268.
36 D. S. Youngblood, S. A. Hatlevig, J. N. Hassinger, P. L. Iversen and H. M. Moulton, *Bioconjugate Chem.*, 2007, **18**, 50–60.
37 C. Samori, H. Ali-Boucetta, R. Sainz, C. Guo, F. M. Toma, C. Fabbro, T. da Ros, M. Prato, K. Kostarelos and A. Bianco, *Chem. Commun.*, 2010, **46**, 1494–1496.
38 S. Varum, A. S. Rodrigues, M. B. Moura, O. Momcilovic, C. A. t. Easley, J. Ramalho-Santos, B. Van Houten and G. Schatten, *PLoS One*, 2011, **6**, e20914.
39 C. F. Chin, S. Q. Yap, J. Li, G. Pastorin and W. H. Ang, *Chem. Sci.*, 2014, **5**, 2265–2270.
40 S. Elmore, *Toxicol. Pathol.*, 2007, **35**, 495–516.
41 I. Vermes, C. Haanen, H. Steffens-Nakken and C. Reutelingsperger, *J. Immunol. Methods*, 1995, **184**, 39–51.
42 S. L. Yoong, B. S. Wong, Q. L. Zhou, C. F. Chin, J. Li, T. Venkatesan, H. K. Ho, V. Yu, W. H. Ang and G. Pastorin, *Biomaterials*, 2014, **35**, 748–759.
43 L. Wei, Y. Zhou, Q. Dai, C. Qiao, L. Zhao, H. Hui, N. Lu and Q. L. Guo, *Cell Death Dis.*, 2013, **4**, e601. Available from URL: http://www.ncbi.nlm.nih.gov/pubmed/23598413.
44 N. Y. Fu, S. K. Sukumaran, S. Y. Kerk and V. C. Yu, *Mol. Cell*, 2009, **33**, 15–29.
45 S. K. Sukumaran, N. Y. Fu, C. B. Tin, K. F. Wan, S. S. Lee and V. C. Yu, *Mol. Cell*, 2010, **37**, 768–783.
46 N. Y. Fu, S. K. Sukumaran and V. C. Yu, *Proc. Natl. Acad. Sci. U. S. A.*, 2007, **104**, 10051–10056.